



# Heat-conducting properties of thermobarically-sintered detonation nanodiamond

V. A. Plotnikov<sup>1</sup>, D. G. Bogdanov<sup>†,1</sup>, A. S. Bogdanov<sup>1</sup>, A. A. Chepurov<sup>2</sup>, S. V. Makarov<sup>1</sup>,  
A. P. Yelisseyev<sup>2</sup>, E. I. Zhimulev<sup>2</sup>, V. G. Vins<sup>3</sup>

<sup>†</sup>bogdanov.d.g@mail.ru

<sup>1</sup>Altai State University, Barnaul, 656049, Russia

<sup>2</sup>V. S. Sobolev Institute of Geology and Mineralogy SB RAS, Novosibirsk, 630090, Russia

<sup>3</sup>VELMAN Ltd, Novosibirsk, 630060, Russia

The research was conducted to study the thermal conductivity of detonation nanodiamonds-based composites. Composite nanodiamond materials were obtained in the course of thermobaric sintering at the press-free high-pressure apparatus (BARS) under 5 GPa and at temperatures within the range of 1100–1500°C. It was ascertained that unlike diamond monocrystals with their thermal conductivity reaching up to 2100 W/(mK), the thermal conductivity of a nanodiamond composite is considerably lower and does not go beyond 18 W/(mK). Specifically, the temperature dependence of the thermal conductivity coefficient of a nanodiamond composite is anomalous as compared to a similar dependence in diamond monocrystals. The thermal conductivity coefficient in diamond monocrystals grows in compliance with the rising temperature, whereas it shows practically no changes in a nanodiamond composite in the temperature range of 50–300°C. Such a temperature dependence of the thermal-conductivity coefficient is apparently related to the features of the phonon spectrum of diamond monocrystals. This feature is stipulated by the dependence of the phonon spectrum of nanocrystals on their size, represented by a set of phonon modes in the range of the wave vector  $0 < q < 1/L$ , i.e., the size of a diamond nanocrystal of 4.5 nm is alleged to limit the excitation of harmonics during nanodiamond composite heating, as opposed to macroscopic crystals that demonstrate the excitation of higher-frequency phonon modes during temperature growing.

**Keywords:** detonation nanodiamond, thermobaric sintering, thermal conductivity, Raman spectra.

## 1. Introduction

Among the unique features of diamond materials, there are high hardness, which can reach 80–130 GPa in some types of diamond [1], and high thermal conductivity, reaching 2200 W/(mK) in diamond single crystals [2]. The total assembly of these features makes it possible to consider diamond as a promising material for obtaining robust composite materials and efficient heat-sinking panels designed for increased thermal and mechanical loads. Increasing density of active elements in integrated circuits followed by extensive heat emission localized within small volumes requires finding the solution. This task demands creation of heat-removing materials with a thermal conductivity over 400 W/(mK) [3].

Currently, the creation of diamond substrates with high heat-conductive properties and the required dimensions is a challenge. The thermal conductivity of a diamond microsize particle-based composite material is conditioned by the regular mechanism of phonon scattering. As for diamond nanoparticle-based composites, here the motion of phonons is quasi-ballistic and it is the boundary, or, more exactly, interfacial phonon scattering that is the major factor in reducing thermal conductivity [4]. Composite substrates made of nano- and microcrystals give no solution to the problem so far [5].

One of the possible ways to solve the problem is the development of diamond composite materials at high temperatures and under high pressures using metallic and non-metallic binders [3, 6, 7]. Normally, sintering of diamond particles at high pressures and temperatures results in an increase in the thermal conductivity. It is characteristic that the observed increase in the thermal conductivity of copper-diamond metal-diamond composite up to 900 W/(mK) is associated with the use of diamond grains as small as several hundred microns in size (200  $\mu$ m and more) and with the formation of a diamond scaffold [8, 9, 10]. The use of silicon as an ingredient in a nanodiamond-silicon blend makes it possible to obtain robust diamond-containing materials with a microhardness reaching 70 GPa just due to formation of diamond scaffold [6]. The formation of a diamond scaffold apparently occurs by means of silicon-carbide at the boundary of adjacent nanocrystals. It is stated that thermal conductivity of composites obtained by sintering diamond particles 100–50  $\mu$ m in size with a copper or silvery binder containing carbide-promoting boron, chromium, or silicon additives, can attain 640–970 W/(mK) [7].

The extremely low thermal conductivity of detonation nanodiamond (5–7 W/(mK)) puts limitations to its use for heat-conducting substrates [11]. As was stated above, such a low value of the thermal conductivity coefficient [4] relates to

the heat scattering mechanism in transition from diamond microparticles to nanoparticles in thermobarically sintered material.

Yet, the study of the heat-conducting properties of a nanodiamond composite makes it possible to reveal features of the phonon spectrum of detonation diamond nanoparticles, that affect its thermal conductivity. That is, the study of nanodiamond composite materials obtained by thermobaric sintering of detonation diamond is an urgent task not only for the formation of a diamond scaffold under high pressures and at high temperatures [12], but also for getting new data on the mechanism of heat conductivity of the composite.

## 2. Materials and experimental methods

Detonation nanodiamond powder produced by Federal Research & Production Center Altai in compliance with technical specification 84-1112-87 was used in the research. Thermobaric sintering of nanodiamonds was fulfilled on a high-pressure multi-anvil “split-sphere” apparatus (BARS) in accordance with the state assignment to the Institute of Geology and Mineralogy the Siberian Branch of the Russian Academy of Sciences. The high-pressure cell was made of refractory oxides  $ZrO_2$  and  $CaO$  with a tubular graphite heater. Delivery of the electrical current to the heater was ensured through molybdenum contacts. Instrument errors in measuring pressure and temperature were taken as  $\pm 0.2$  GPa and  $\pm 25^\circ C$ , respectively. The experimental mode was the following: pressure increasing, heating the sample under study, 60-second exposition and quick cooling. The quenching time made 2–3 seconds determined by the effective water cooling of the inner punch stage of the BARS apparatus. The pressure was detected by a curve showing the dependence of the pressure in the cell on the outer pressure upon the multi-anvil block of the BARS apparatus. Sintering was executed under a pressure of 5 GPa and at temperatures of 1100, 1200, 1300, 1400 and 1500°C. To conduct experimental thermobaric sintering, disks 8 mm in diameter were made from the detonation nanodiamond initial powder. Then capsules of refractory  $MgO$  oxide were fabricated. Before starting the experiment, the sample was put into the capsule to be dried at 120°C. The application of this method provided sintering of a sample a volume of more than 250 mm<sup>3</sup>. After the sintering procedure, the capsule was dissolved in concentrated  $HNO_3$  to release the sample. The features of the apparatus design and details on the applied experimental methods were described in detail in [13].

Thermobaric sintering of metal-diamond composites was carried out under a pressure of 4 GPa and at a temperature of 1300°C to compare the heat-conducting properties of diamond materials. Natural diamond powders with a particle size of about 300  $\mu m$  and synthetic diamond powder with a particle size of 30–40  $\mu m$  were used as a diamond blend. Copper powder was applied as a metallic ingredient. Diamond and copper were mixed and placed into a capsule made of a mixture of refractory oxides. Powder diamond and monocrystals were provided by the Institute of Geology and Mineralogy the Siberian Branch of the Russian Academy of Sciences (SB RAS).

The TM- $\lambda$ -400 apparatus was applied to measure the thermal conductivity of diamond materials. The unit is intended for assessing the dependence of thermal conductivity

on the temperature of solid bodies in the monotonous heating mode. A material with initially-known thermal conductivity (copper) was used to grade and calibrate the measuring cell. Precise matching of the size and shape of the fabricated copper samples to the similar parameters of the sintered diamond and metal-diamond composite materials was made to ensure accurate calibration and measuring adjustment due to the size of the examined samples. Prior to each measuring episode, the contact area and the element itself were carefully cleaned from impurities and oxides. More details of the methodical specifics are presented in the paper [14].

Raman spectra were obtained at the Institute of Geology and Mineralogy SB RAS at room temperature a confocal Raman microspectrometer LabRAM HR800 with excitation by a He-Cd gas laser (325 nm) and the solid-state laser second harmonics at Nd:YAG with diode pumping (532 nm).

Figure S1 (supplementary material) gives the chart that explains the equipment and methods used in the experiments.

## 3. Results and discussion

Figure 1 shows the dependence of the thermal conductivity coefficient on the temperature for five thermobarically sintered detonation nanodiamond samples under a pressure of 5 GPa and at temperatures of 1100, 1200, 1300, 1400, 1500°C.

As follows from Fig. 1, the thermal conductivity of the samples obtained as a result of thermobarically sintered detonation nanodiamonds lies within the range of 7–19 W/(mK) at 50°C, and within the range of 10–17 W/(mK) at 300°C, indicating minimum changes. However, the dependence of the thermal conductivity coefficient on the temperature is not monotonic. Greater thermal conductivity fluctuations are observed in the temperature range of measurements about 100–200°C, with the extreme value surpassing the average level approximately by 1.5 times.

Meanwhile, the dependence of the thermal conductivity of diamond monocrystals on temperature indicates a regular classical pattern, i.e. the thermal conductivity shows monotone growth with rising temperature (Table 1).

Table 1 gives data on measuring thermal conductivity coefficient of a high-quality diamond monocrystal and of a monocrystal synthesized in catalytic medium Fe-Ni-C within the temperature range 50–250°C.

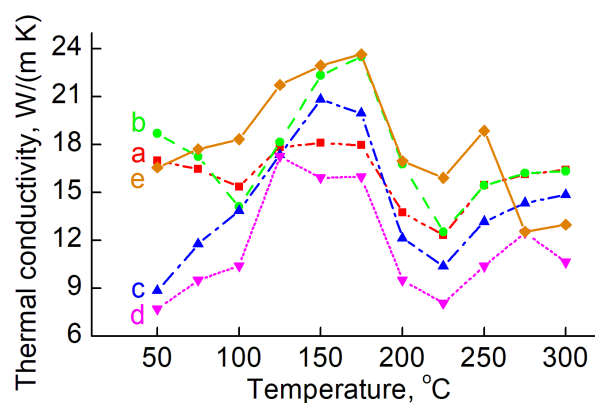


Fig. 1. (Color online) Thermal conductivity coefficients of thermobarically sintered detonation nanodiamonds within the temperature range 50–300°C: 1100 (a), 1200 (b), 1300 (c), 1400 (d), 1500°C (e).

As the data in Table 1 indicate, the thermal conductivity of high-quality monocrystal (Fe-Al-C system) is high and makes about 2089 W/(mK) at 50°C, whereas the thermal conductivity of synthesized crystal (Fe-Ni-C system) is sufficiently lower — 606.7 W/(mK). But the dependence of the thermal conductivity coefficient on temperature is about the same — with the measuring temperature growing up to 250°C, the thermal conductivity of both monocrystals demonstrates similar monotone growing.

The high value of the thermal conductivity coefficient in a high-quality diamond crystal (Fe-Al-C system) and the similarly monotone pattern of the dependence of the thermal conductivity coefficient on temperature in the synthesized monocrystal (Fe-Ni-C system) prove the classical phonon mechanism of thermal conductivity in both monocrystals. The decrease in the value of thermal conductivity in a monocrystal synthesized in the Fe-Ni medium occurs, apparently, due to the impact of impurity atoms upon the scattering of phonons. The integrated data on the thermal conductivity coefficient of our materials shown in Table 2 give a distinct picture of the specific process of heat transfer depending on the size of the diamond particles forming the composite material. That is, the impact of the boundaries upon phonon scattering obviously manifests itself in the succession of values of thermal conductivity of a diamond monocrystal (Fe-Al-C system), diamond monocrystal (Fe-Ni-C system), metal-diamond composite and thermobarically sintered detonation diamond. While the impact of scattering in a diamond monocrystal is minimum at the boundaries, the sintered detonation diamond with a size of a nanocrystal of about 4.5 nm [15] demonstrates the maximum impact of the boundaries upon scattering. The quasi-ballistic character of the motion of phonons in diamond nanocrystals [4] and the anomalously high specific surface of the boundaries that reaches 300 m<sup>2</sup>/g [16], give grounds to conclude that the scattering material plays a dominant role in the formation of thermal resistance at the boundaries.

Table 2 shows a significant dependence of the thermal conductivity of diamond materials on their structural state,

mostly on impurity atoms and boundaries. As for the thermal conductivity of the metal-diamond composite, in which the diamond constituent is formed by micron-sized crystals within the range of 30–300 μm, it is close to the thermal conductivity of a synthetic monocrystal (Fe-Ni-C system). That means that the mechanism of the thermal conductivity in the metal-diamond composite is stipulated by phonons, and somewhat lower value of the thermal conductivity coefficient is due to the presence of a metallic binder between adjacent crystals. This explains the value of the effective thermal conductivity coefficient in Table 2 that is dependent on the correlation of the metallic and diamond constituents of the composite [3,7]. It is noteworthy that a certain contribution can be made by the specific relief of the surface of diamond microcrystals. This surface pattern can get substantial changes in case of interaction with the matrix material, especially in the presence of transition metals [17]. The considerably lower (by an order of magnitude lower) value of the thermal conductivity of the thermobaric sintered nanodiamond composite, as compared to the thermal conductivity of a diamond monocrystal emphasizes the predominance of scattering at the boundaries.

The anomalous dependence of the thermal conductivity coefficient on temperature within the temperature range of 50–300°C of the nanodiamond composite is remarkable, indicating practically no changes and fluctuating around 18 W/(mK). This feature of the thermal conductivity coefficient dependence on temperature is quite clear from the analysis of the Raman-spectra of the detonation nanodiamond initial powder (Fig. 2) and sintered nanodiamond composites (Fig. 3).

In the Raman-spectrum of detonation nanodiamond (see Fig. 2) in addition to the diamond line of about 1322 cm<sup>-1</sup> there is another line of about 1600 cm<sup>-1</sup>, belonging to the carbon of the diamond core graphite shell. Meanwhile, the diamond line 1322 cm<sup>-1</sup> in the Raman-spectra of the sintered detonation nanodiamond is not observed. The marked lines about 1600 and 1380 cm<sup>-1</sup> belong to the carbon of non-diamond phase, the first one belongs to the graphite (G-line), the second (D-line) — to the so-called (disordered graphite [18]) respectively.

**Table 1.** Thermal conductivity of diamond monocrystals.

Temperature, °C	Thermal conductivity coefficient λ, W/(mK)	
	Diamond monocrystal synthesized high-quality (Fe-Al-C system)	Diamond monocrystal synthesized (Fe-Ni-C system)
50	2089.0	606.7
75	1806.8	607.1
100	1739.6	584.0
125	2158.7	598.0
150	2334.1	681.9
175	2398.6	690.6
200	1956.2	717.4
225	2008.4	817.1
250	2271.3	744.7
Mean	2106.4	671.9

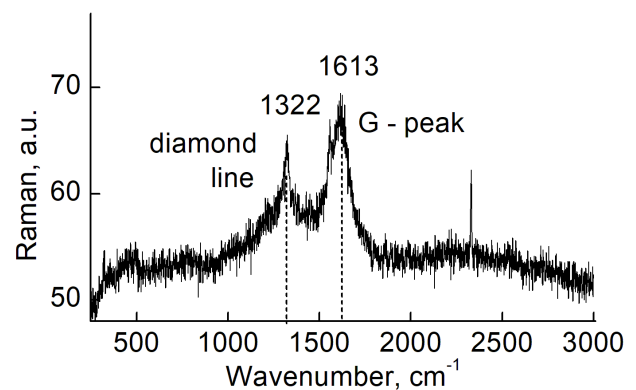


**Fig. 2.** Raman-spectrum of detonation nanodiamond initial powder. In addition to the diamond line 1322 cm<sup>-1</sup> there is another line of about 1600 cm<sup>-1</sup>, linked to the diamond core graphite shell.

**Table 2.** Thermal conductivity of diamond materials.

Thermal conductivity coefficients of various diamond materials, W/(mK)			
Diamond monocrystal (Fe-Al-C system)	Diamond monocrystal (Fe-Ni-C system)	Micron diamond powder-based metal-diamond composite	Detonation nanodiamond-based composite
2089	606.7	485.6	9–18

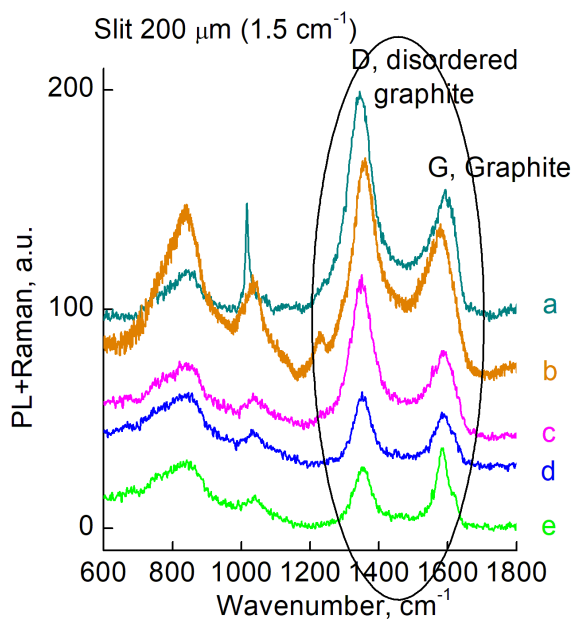


**Fig. 3.** (Color online) Raman-spectra of the sintered detonation nanodiamond at temperatures: 1100 (a), 1200 (b), 1300 (c), 1400 (d), 1500°C (e).

Yet, the absence of the line  $1322\text{ cm}^{-1}$  in the Raman-spectra of thermobaric sintered detonation diamond does not indicate that it is absent in the spectra of combination scattering, since it can be hidden inside the D-line. In fact, in accordance with the effect of confinement on phonon modes [19–21], diamond nanocrystals make the contribution of phonons with wave vectors  $0 < q < 1/L$  into the phonon spectrum quite visible.  $L$  stands for the size of diamond nanocrystals. In this respect, the combination scattering spectrum is widening and shifting to the low-frequency area, and the intensity of line  $1322\text{ cm}^{-1}$  shows a remarkable decrease. The phonon spectrum demonstrates greater dependence on the nanodiamond crystal size due to the extreme values of the wave vector than on the temperature. This is a determining factor that makes the thermal conductivity coefficient of the nanodiamond composite independent of temperature.

#### 4. Conclusions

It is shown that the thermal conductivity of diamond materials in the transition from monocrystals to nanostructured nanodiamond composites declines two orders down due to a change in the dominant factor that contributes to the thermal resistance — phonon scattering upon inner defects is changed by the predominance of phonon scattering at boundaries. The independence of the thermal conductivity coefficient on temperature in the temperature range of 50–300°C is determined by the features of the phonon spectrum in detonation diamond nanocrystals, where it features a set of modes with wave vectors limited by a geometric parameter inverse to the size of nanocrystal. Some increase in the thermal conductivity coefficient of the thermobaric sintered detonation nanodiamond as compared to the established data seems to be stipulated by the scaffold formation of detonation diamond nanoparticles.

**Supplementary material.** The online version of this paper contains supplementary material available free of charge at the journal's website ([lettersonmaterials.com](http://lettersonmaterials.com)).

**Acknowledgements.** The experiments under high pressure were conducted with grant support of the Russian Science Foundation № 21-17-00082. The research work was supported by the Strategic Academic Leadership Program of the Federal State Budget Educational Institution of Higher Education “Altai State University”, “Prioritet 2030”.

#### References

1. H. Sumiya, N. Toda, S. Satoh. *Diamond & Related Materials*. 6, 1841 (1997). [Crossref](#)
2. J.R. Olson, R.O. Pohl, J.W. Vandersande, A. Zoltan, T.R. Anthony, W.F. Banholzer. *Phys. Rev. B*. 47, 14850 (1993). [Crossref](#)
3. E.A. Ekimov, N.V. Suetin, A.F. Popovich, et al. *Inorg Mater*. 44, 224 (2008). [Crossref](#)
4. F.M. Shakhov, A.P. Meilakhs, E.D. Eidelman. *Tech. Phys. Lett.* 42, 252 (2016). [Crossref](#)
5. S.V. Kidalov, F.M. Shakhov, A.Ya. Vul. *Diamond & Related Materials*. 17, 844 (2008). [Crossref](#)
6. E.A. Ekimov, E.L. Gromnitskaya, D.A. Mazalov, et al. *Phys. Solid State*. 46, 755 (2004). [Crossref](#)
7. A.M. Abyzov, S.V. Kidalov, F.M. Shakhov. *Phys. Solid State*. 54, 210 (2012). [Crossref](#)
8. K. Yoshida, H. Morigami. *Microelectronics Reliability*. 44, 303 (2004). [Crossref](#)
9. L. Weber, R. Tavangar. *Adv Mater Res*. 59, 111 (2009). [Crossref](#)
10. G. Bai, N. Li, et al. *Journal of Alloys and Compounds*. 735, 1648 (2018). [Crossref](#)
11. S.V. Kidalov, F.M. Shakhov, A.Ya. Vul, A.N. Ozerin. *Diamond & Related Materials*. 19, 976 (2010). [Crossref](#)
12. P.A. Vityaz, V.T. Senyut. *Phys. Solid State*. 46, 764 (2004). [Crossref](#)
13. A.A. Chepurov, V.M. Sonin, J.M. Dereppe, E.I. Zhimule, A.I. Chepurov. *Eur. J. Mineral*. 32, 41 (2020). [Crossref](#)
14. A.S. Bogdanov, V.A. Plotnikov, A.P. Eliseev, V.G. Vins. Method for obtaining a material of high thermal conductivity and a heat sink made of a material obtained by this method. Patent RU № 2757042. 11 November 2021. (in Russian)
15. D.G. Bogdanov, V.A. Plotnikov, A.S. Bogdanov, et al. *International Journal of Refractory Metals & Hard Materials*. 71, 101 (2018). [Crossref](#)
16. E.M. Baitinger, E.A. Belenkov, M.M. Brzhezinskaya, et al. *Phys. Solid State*. 54, 1715 (2012). [Crossref](#)
17. A.I. Chepurov, V.M. Sonin, A.A. Chepurov, et al. *Inorg Mater*. 47, 864 (2011). [Crossref](#)
18. F. Tuinstra, J.L. Koenig. *J. Chem. Phys.* 53, 1126 (1970). [Crossref](#)
19. S.N. Mikov, A.V. Igo, V.S. Gorelik. *Phys. Solid state*. 37, 3033 (1995). (in Russian)
20. M.J. Lipp, V.G. Baonza, W.J. Evans, H.E. Lorenzana. *Phys. Rev. B*. 56, 5978 (1997). [Crossref](#)
21. J.W. Ager, D.K. Veirs, G.M. Rosenblatt. *Phys. Rev. B*. 43, 6491 (1991). [Crossref](#)